Nagaraju *et al.*
Journal of Engineering and Applied Science (2023) 70:124
https://doi.org/10.1186/s44147-023-00294-6

Journal of Engineering and Applied Science

RESEARCH Open Access

Wear behaviour of hybrid (boron carbide-graphite) aluminium matrix composites under high temperature

Sharath Ballupete Nagaraju[1*], Madhu Kodigarahalli Somashekara[1], Pradeep Dyavappanakoppalu Govindaswamy[1], Madhu Puttegowda[1], Premkumar Bagade Girija Shankar[1] and Karthik Sathyanarayana[2]

*Correspondence: sbn@mcehassan.ac.in

[1] Department of Mechanical Engineering, Malnad College of Engineering, Hassan, Affiliated to VTU, Belagavi, Karnataka, India
[2] Department of Research and Development, REVA University, Bengaluru, Karnataka, India

Abstract

Aluminium MMCs are among the many metal composites and are regarded as progressive engineering materials in numerous industries because of their advantages compared to standard aluminium alloy. Among the reinforcements in MMCs, ceramic particles are preferred for their superior wear resistance, temperature resistance, and adhesion to their matrix, making them a popular choice. This research work has been carried out to synthesise ceramic particle-reinforced aluminium metal matrix composites and to evaluate their tribological properties at different temperatures (50–300℃). Al2618 alloy was selected as the matrix, and boron carbide (B_4C) and graphite (Gr) were selected as reinforcements. Hybrid composites are prepared through stir casting by varying the wt.% of B4C and Gr reinforcement particles with a ratio of 3:2. Microstructural observation shows the uniform distribution of B4C and Gr particles throughout the matrix without any agglomeration, and it also exhibits excellent scanning electron microscope (SEM). X-ray diffraction analysis (XRD) was performed to verify the presence of different constituents in the developed material. Samples S4 (Al 2618 + 12 wt.% B4C—8 wt.% Gr) and S5 (Al 2618 + 15 wt.% B_4C—10 wt.% Gr) exhibit enhanced wear resistance (16.45%) due to the incorporation of a higher quantity of Gr solid lubricants alongside B_4C within the temperature range of 50 to 300℃. The thickness and stability of the glazed layer exhibited adequate resistance to wear.

Keywords: B_4C, Gr, Al2618, Delamination wear, Glazed layer

Introduction

The development and prosperity of civilizations have often been closely linked to their members' expertise to produce and use materials to fulfil their needs. Metallic and non-metallic materials have traditionally been used to build a laminated structure in earlier civilizations. Perhaps the history of modern-day composites begins in the nineteenth century. The invention of polymer-based composites in 1960 spurred industrial use by

numerous industries. Plastics, ceramics, and composites have become the most prevalent new materials since the early 1960s. The use of composite materials has evolved rapidly, entered new markets, and conquered them. New composite structures represent a major part of the demand for manufactured goods, from everyday items to heavy machinery. Composites have since been known as superior materials and are designed and manufactured for a wide range of industrial and non-industrial applications, including the aircraft and automotive sectors. At the start of the 1980s, efforts were undertaken to produce (MMC) metal matrix composites from aluminium alloys using SiC whisker reinforcements. The fundamental purpose was to significantly boost aluminium alloys' properties by obtaining extremely precise strength and resistance, but the whiskers' cost was quite high. The research goal was to exploit low-cost and low-density strengthening at the beginning of the twenty-first century. Composite materials are one such multi-phase material, obtained by the mixture of various materials to achieve properties that the individual materials cannot acquire on their own [1, 2]. Industries today are under tremendous pressure to propose new cost-effective materials for their products. The usage of aluminium-based MMCs has recently received increasing attention from the aerospace and transportation industries due to their higher specific heat capacity, outstanding thermal conductivity, excellent abrasion resistance, and negligible assault by fuels and solvents. One of the most important factors in the development of high-performance MMCs is having the capability to endure applied stress by transforming the load from the matrix to the reinforcing phase. It helps to withstand the required load, but artificial composite (polymer) structures are seldom suitable for these limitations. Despite the massive growth, technical challenges exist in producing MMCs based on aluminium from the last decade. Ceramic reinforcements can be introduced in continuous fiber, short fiber, whisker, or particle form. Besides, ceramic-reinforced AMMCs (aluminium metal matrix composites) exhibit superior strength and stiffness, creep resistance, and superior frictional and wear resistance. Notably, it has a low weight ratio compared to conventional materials. Thus, these AMMCs have arisen for tribological applications as a promising material, including brake rotors and drums, cylinder liners, and pistons [3, 4]. In earlier days, in view of more restrictive constraints regarding emissions of exhaust fumes, automobile manufacturers had decided to cast light metals to lower the engine weight and lower fuel usage. As a result of the foregoing, Al-silicon (Si) alloys were first utilised to make engine components such as cylinder heads and cylinder blocks. Resistance to abrasive wear and seizures had long been a major issue with Al-Si alloy-based cylinder liners. The heat is dissipated more quickly and uniformly in Al-Si-made engine blocks. As a result, the cooling system requires less coolant. High stability of the piston could be maintained irrespective of the operating circumstances of the engine due to the identical thermal expansion coefficient of the piston and cylinder liners. Hence, the lack of adequate information for understanding concerns the extremely favourable cast microstructure of cylinder liners. The cylinder bearing surface profile's geometrical parameters secure sufficient retention of lubricant. The information available in this area is confined to cast iron liners [5]. Aluminium metal matrix composites (MMCs) are a category of metal composites that are widely recognised as advanced engineering materials in various industries due to their superior properties in comparison to conventional aluminium alloys. Ceramic particles are commonly used as

reinforcements in metal matrix composites (MMCs) due to their exceptional wear resistance, temperature resistance, and strong adherence to the matrix material. As a result, they have gained significant popularity in the field. Particulate composites are easy to process as compared with fibre-reinforced composites and are nearly isotropic. Distributions of particle reinforcement are dependent on the fabrication method. MMCs are made using a variety of techniques, and the most potent of which is traditional stir-casting. The way this is done makes sure that the material for reinforcing is spread out evenly throughout the matrix, as a result of which it forms excellent interface bonding with the composite [6]. Al6061-T6 and Al6061-20% Al_2O_3-T6 composites are prepared by the extrusion process. Reinforced alloys possess more hardness than unreinforced alloys meanwhile more strength and wear resistance. Initially, a higher rate was noted, but resistance was enhanced at 150℃. Severe wear is caused by large plastic deformations that involve the recrystallization of extensively deformed sub-surface grains. The development of a tribo-layer composed of finely dispersed $A1_2O_3$ particles increases the wear resistance of AMMCs [7]. The 2014-MMC and 6061-MMC were prepared using 17% and 20% volumes of Al_2O_3, respectively. The 2014-MMC has superior ultimate tensile strength (UTS) compared to the 6061-MMC at various temperatures (25℃, 93℃, 150℃, and 200℃) due to the exceptional uniformity of reinforcement dispersion inside the Al2014. The observation has been made that variations in test temperature do not seem to exert a significant influence on the material's failure [8]. The composite material consisting of Al6061-20% Al_2O_3 exhibits superior strength compared to the composite material including Al6061-10% Al_2O_3 throughout all temperature ranges. The mechanical integrity of the reinforced alloy exhibits a decline as the temperature rises, and this pattern is also observed in both composites. The 2014-MMC and 6061-MMC were prepared using 17% and 20% volumes of Al_2O_3, respectively. The 2014-MMC has superior ultimate tensile strength (UTS) compared to the 6061-MMC at various temperatures (25℃, 93℃, 150℃, and 200℃) due to the notable uniformity of reinforcement dispersion inside the Al2014. The observation has been made that variations in test temperature do not seem to exert a significant influence on the material's failure [9]. The Al-5% Mg alloy was made using the stir casting procedure with the addition of 20 wt.% B4C. The observed trend indicates a consistent drop in hardness values as temperature increases. The use of 20 wt.% B4C results in a marginal increase in the transition temperature, elevating it from 262 to 274 ℃. The phenomenon of interatomic distance expansion, which occurs as a result of elevated temperatures, can be attributed to structural deformations [10]. Powder metallurgy techniques were utilised in the development of Metal Matrix Composites (MMCs), with subsequent assessment of wear characterisation conducted throughout a range of temperatures spanning from 100 to 450 ℃. Based on microstructural tests conducted using scanning electron microscopy (SEM), it has been observed that the presence of a uniform graphene (Gr) layer on a worn surface leads to a decrease in plastic deformation. The use of Gr particles as an effective additive for copper-based metal matrix composites (MMCs) at elevated temperatures was observed [11]. The spray deposition method has been employed in the fabrication of advanced metal matrix composites (AMMCs). The experimental procedure involved conducting uniaxial stress tests within a range of strain rates ($\varepsilon = 0.001$ to 0.1 $s-1$) at temperatures ranging from 573 to 723 °K. The results indicate that strain softening persists till the point of rupture and that

the flow stress exhibits a direct relationship with the strain rate while decreasing with increasing temperature. The extent of elongation shown by AMMCs is contingent upon both temperature and strain rate [12]. As the hardness of the mating surface increases, there is a corresponding increase in the friction coefficient value at elevated temperatures. The management of glazing layer production is contingent upon the various forms of wear. The aforementioned levels possess distinct functions within their respective failure mechanisms [13]. The fabrication process of a fly ash-reinforced composite involved the use of powder metallurgy and hot extrusion methods. Even when the temperature reached 573 °K, there was no observable transition from mild to severe wear. The particle hardness of the sub-surface layer exerts a significant impact. The Al6061-T6-based AMMCs have exhibited enhanced wear resistance in comparison to untreated Al6061-based AMMCs [14]. The Al-4Cu and Al-4Cu-TiB2 composites were fabricated using the in situ technique. The composite material augmented with TiB2 exhibits enhanced wear resistance. Severe wear was seen at a temperature of 300 ℃, which can be attributed to the presence of titanium diboride (TiB2) [15].

From the literature survey, it is understood that early investigations were made on an Al-based matrix with ceramic reinforcement composite materials. It shows that mechanical properties were correlated with base alloy and varying reinforcement material. A considerable number of studies concentrate mainly on room temperature properties evaluation. In practice material developed is subjected to a high-temperature environment. Thus, it is another gap that needs immediate attention for the researcher to work on. In the deliberation of engineering applications, additional attention has been paid to study the wear properties of hybrid composite materials. The majority of failures in automotive parts and tribological components can be attributed to the wear process, especially at elevated temperatures. Hence, a study of tribological components at elevated temperatures is found to be more appropriate. Wear and tensile deformation are influenced by microstructure inhomogeneities and the presence of precipitates. Hence, to tailor the material for good tribological performance, there is a need for a fundamental understanding of the influence of microstructure on tribological and mechanical properties. In this regard, the topic that this particular study is going to concentrate on fabricating a hybrid composite (Al2618) by reinforcing B_4C and Gr to overcome the drawbacks of Al-Si alloy concerning undesirable microstructure for high-temperature applications.

Wear characteristics of the hybridised composite and unreinforced Al2618 can be more precisely determined by using L18 orthogonal array (Taguchi model). The samples were subjected to wear tests at different temperatures (50 to 300 ℃) to learn more about their properties. SEM and XRD were used to analyse the microstructure and phase composition.

Materials and methods

Al2618 was utilised as a matrix and its ingot form is depicted in Fig. 1. Cu is the prominent alloying ingredient and lies between 5.8 and 6.8% and is combined with a lower 0.01–0.02% Mg leading to thermal treatable alloy. Table 1 provides the chemical composition of alloy Al2618. When Si and Mn are added in minor quantities, these alloys are ideal for medium to high-strength applications. Heat treatment can be done to modify

Fig. 1 Stir-casting steps

Table 1 Constituents of Al2618 [17]

Element	Si	Fe	Cu	Mn	Mg	Cr	Ni	Zn	Ti	B	Ca	Al
Wt. %	0.24	1.30	2.52	0.004	1.46	0.02	1.14	0.01	0.07	0.003	0.002	Balance

strength, but with inadequate ductility. Al2618 is an alloy selecting the precise alloy for a given application, and it entails consideration of better strength and good damage tolerance properties obtained in different circumstances at high temperatures as well as very low temperatures. Al2618 is ideal for manufacturing engine blocks. Al2618 have a lower resistance to stress corrosion and cracking; thus, they are frequently employed in a little overaged temper to provide a better balance of strength, fracture toughness, and corrosion resistance [16].

Boron carbide (B_4C) is well recognised ceramic and dispersion in AMMCs contributes significantly to increased stiffness and wear resistance. Due to its exceptional hardness (just below that of diamond: 2900–3580), B_4C particles are used to reinforce the matrix and have exceptional hardness and fracture resistance. It is essentially non-semiconductive and resilient at high temperatures. It has a low density of 2.52 g/cm^3 and exceptional thermal conductivity (30–42 W/m °K). It has a Rhombohedral crystal structure and melts at a temperature of 2450 ℃. B_4C is identified as a substantial strengthening for tribological application; moreover, it might be a substitute option for SiC-based AMMCs in applications requiring high stiffness and superior wear resistance. The addition of B_4C alone is not beneficial in larger quantities, hence requiring further strengthening. AMMCs have long been known to lead to significant gains in stiffness and wear resistance. Enviable properties of graphite are high strength and greater chemical stability at high temperatures and excellent thermal conductivity, so it is generally useful for high-temperature applications and offers outstanding mechanical properties. In addition, Gr

has a self-lubricating feature that aids in the reduction of wear in tribological components. Gr improves the machinability of the composite, and it is also low density (2.23 g/cm^3) material leads to reduce the mass of the composite. So far, the research that has been done on the topic of hybridisation's potential to enhance the physical properties of MMCs has been promising [18–23]. The primary objectives of this study are to improve the wear resistance of Al2618 metal matrix composites by using a suitable mix (Table 2). As a result of its unique ceramic composition, this Opticritter alloy can provide improved tribological performance.

Fabrication of composites using stir casting method

To manufacture specimens having various wt.% of B_4C and Gr (3:2), optimal process parameters were chosen by employing a stir casting process at a room temperature. In this process, the particles are stirred into an aluminium melt and the mixture is subsequently solidified in the mould under atmospheric pressure. Al2618 based-composite was prepared using a stir-casting process, an electric melting furnace with a graphite crucible was used for melting under normal atmospheric conditions. Al2618 alloy was melted in a crucible at 750 ℃ for 1.5–2 h. The B_4C and graphite particles were heated to 350 ℃ to eliminate humidity and other adhering contaminants; meanwhile, the permanent moulds of cast iron were heated to reduce the effect of chilling during solidification. Coverall (1%) is added to increase the wettability and separation of slag. Magnesium chips are added to increase the wettability. The preheated weighed B_4C particles (50 µm) were incorporated into the melt and thoroughly mixed through a mechanical stirrer for 10–15 min at 150 rpm. Further Gr (graphite) was added into the melt and mixed with the help of a stirrer, and the stirrer is activated for 10–15 min at a speed of 100—150 rpm. The metallic die is filled with mixed molten metal and allowed to solidify under atmospheric pressure [19, 24].

X-ray diffraction and microstructural study

XRD is a technique for examining single-crystal and polycrystalline materials. The samples have been sliced into small discs for the XRD study with a diameter of 10 mm and a width of 2 mm. The diameter of the electron beam utilised to examine the material is less than 0.01 m. Experimental X-ray diffraction was performed using a Cu-K radiation source ($K = 1.54056$) and an advanced goniometer model 2036E201 (Bruker). The

Table 2 Wt.% of B_4C and Gr (3:2)

Sample designations	Composition	Al2618, Wt. %	Boron carbide (B_4C), Wt.%	Graphite (Gr), Wt.%
S	Al 2618	100	0	0
S1	Al 2618 + 3% B_4C–2% Gr	95	3	2
S2	Al 2618 + 6% B_4C–4% Gr	90	6	4
S3	Al 2618 + 9% B_4C–6% Gr	85	9	6
S4	Al 2618 + 12% B_4C–8% Gr	80	12	8
S5	Al 2618 + 15% B_4C–10% Gr	75	15	10

sample was held in one place while a 2°/min scan was performed between a diffraction angle of 10–100° (2θ).

SEM was used to investigate the microstructures of samples. Tiny portions of the specimens were used for microstructural observation. The samples were cut to the dimensional accuracy of 10 mm × 10 mm. The samples have been washed with solvents and then polished by silicon carbide emery (1200, 2000, and 4000 grit). The polished samples were cleaned and engraved with Keller's etchant to prepare for the microscopic studies. SEM was used to assess the dispersion of the reinforcements.

Wear test

Dry sliding wear tests were carried out in accordance with ASTM-G99 requirements utilising pin-on-disc equipment (Manufacturer: Ducom triboinnovators). Cylindrical specimens (10 ϕ × 30 L in mm) were employed as test samples. SiC-emery paper (size: 2000, 4000 μ) was utilised to polish the end surface of the sample before being cleaned with acetone. The 1-μm surface-finished disc of En-32 steel (60 HRC) was employed throughout testing as the counterface. All trials were carried out with a track radius of 120 mm. The sample was attached to a holder that had two jaws, and the specimen was subjected to a load. The arm was used to apply a force to the specimen, which was then balanced by adding a weight. Load (L = 20–60 N), sliding velocity (V = 1.25–3.75 m/s), sliding distance (D = 400–800 m), and temperature (T = 50–300 ℃) were considered while analysing the HMMCs sliding wear behaviour. In the current exploration, the high-temperature wear attributes of the HMMCs are investigated by the pin-heating technique. The sample is retained within the pin holder. A potential differential integral (PDI) instrument has been used for regulating the temperature required in the pin holder and sample. During the test, with the aid of the force transducer, the frictional force was recorded for each trail.

After the test, each sample was ultrasonically cleaned with acetone and the weight loss was measured with an electronic weighing balance (accuracy = 0.0001 mg). Equations 1 and 2 are used to calculate the wear rate and coefficient of friction of reinforced samples and unreinforced samples. For each composition, an average of three trials were recorded.

$$\text{Wear rate } (W) = \text{ weight loss}/(\text{density of the composite } \times \text{ sliding distance}) \quad (1)$$

$$\text{Coefficient of friction } (\mu) = \text{ friction force}/\text{applied load} \quad (2)$$

Results and discussion

Microstructure and x-ray analysis

SEM was used to examine the microstructure and distribution of B_4C and graphite reinforcing particles in the produced HMMCs. SEM images of reinforced HMMCs are displayed in Fig. 2. It demonstrates the existence of B_4C and graphite particles in HMMCs, and the reinforcement particles are appropriately scattered throughout the Al2618 matrix. The HMMCs display an abundant interface between Al2618, B_4C, and graphite particles. The dendrites of Al during solidification are excluded owing to the solid–liquid interface and B_4C and graphite particles act as nuclei agents. A considerable number of

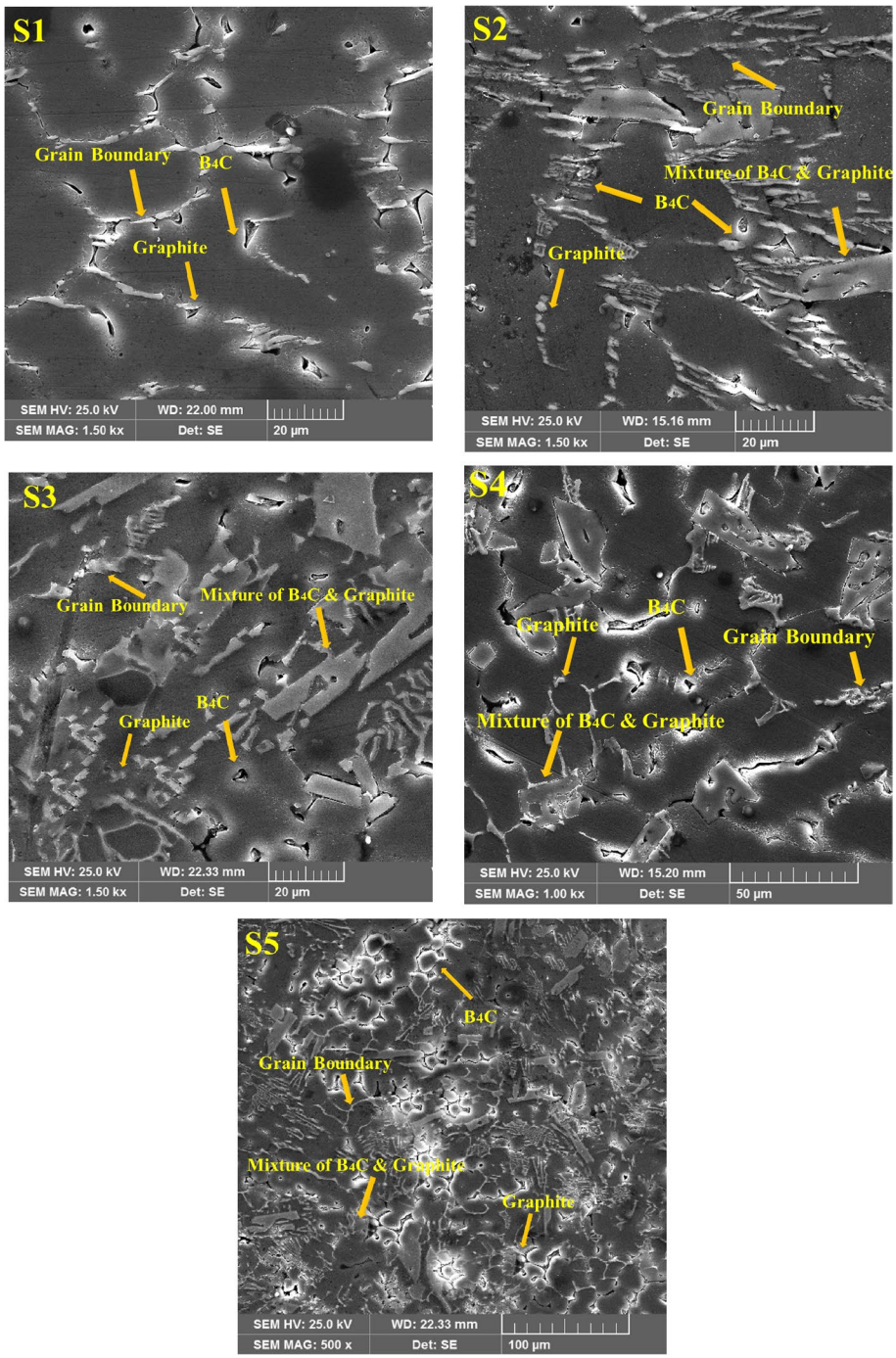

Fig. 2 SEM of sample

nuclear sites near the mould wall influenced the production of partial equi-axie grains, as evidenced in reinforced samples (S1-S5). The degree of supercooling was significantly lowered due to the presence of the mould surface and ceramic particles. The HMMCs also demonstrated that they are free from casting flaws such as porosity, slag inclusion, and shrinkage which can arise during solidification owing to adequate bonding between

the Al2618 matrix and ceramics during solidification. It is emphasised that the composite solidification pattern is a fundamental determinant of particle dispersion in composites. With the rise of strengthening content, the mean space is lowered among the strengthening particles. The outcome is the formation of boundaries. The uniform dispersion of B_4C and graphite in the created HMMCs can be associated with the parameters used in their manufacturing. The HMMC microstructure demonstrates that the stirring technique was responsible for generating a homogenous structure. Indeed, the dispersion of strengthening particles relies on the density gradient between the molten metal and particles. The higher viscosity of the molten metal helps to regulate the vertical motion of strengthening particles. This prevents particles from being immersed in the molten alloy [25, 26].

XRD offers information about the various elements included in the produced HMMCs. Figure 3 (a) depicts an XRD study of Al2618; it demonstrates that the most often available element is Al (higher peaks) and smaller peaks that disclose the additional element Cu. The XRD pattern of HMMCs with a different amount of B4C and graphite particles (3:2) is shown in Fig. 3 (b–f). After introducing B4C and graphite in Al2618, solid peaks were noticed from the XRD pattern and smaller peaks that disclose additional elements such as Mg and Cu.

Density and porosity

The discrepancy in density (ρ) values due to the addition of reinforcement (wt.%) is depicted in Fig. 4. The influence of B_4C and Gr on the densities of the produced HMMCs is investigated empirically using the Archimedes principle. Mixing rule utilised to estimate the ρ_{th} (theoretical density). It is noted that the computed ρ_{exp} values of HMMCs differ from the ρth due to the presence of pores and vacuums. The ρ_{exp} of Al2618 alloy was 2.69 g/cm^3 and is reduced to 2.6 g/cm^3 when wt. % of B_4C and graphite was raised. The inclusion of B_4C and graphite particles in the application of MMCs saves up to 60% owing to the lower density of B_4C (2.52 g/cm^3) and graphite (2.23 g/cm^3) particles.

Figure 5 displays the difference in porosity that occurred in samples. The presence of pores can lead to a reduction in the HMMC's characteristics, both physically and mechanically. Pores and other casting flaws are not taken into account when estimating ρ_{th}. Therefore, it is always higher than ρ_{exp}. The findings demonstrate that the porosity lowered with the inclusion of 3 wt.% B_4C and 2 wt.% graphite. Additional inclusion for porosity is not advantageous but the porosity was within the permissible threshold of 3–6% both for reinforced and unreinforced samples. The S4 sample exhibits lower porosity compared with S5 and S3.

Wear behaviour

Effect of temperature on the wear rate of Al2618 and HMMCs

Figure 6 (a–c) depicts the impacts of temperature on the wear rate of the Al2618 and HMMCs at various conditions for all compositions (L (applied load) = 20, 40, and 60 N; S (sliding speed) = 1.25, 2.5, and 3.75 m/s; D (sliding distance = 800 m)). Figure 6 (a–c) concluded that the prevalence of the wear rate drops as the temperature increases for all samples (S-S5).

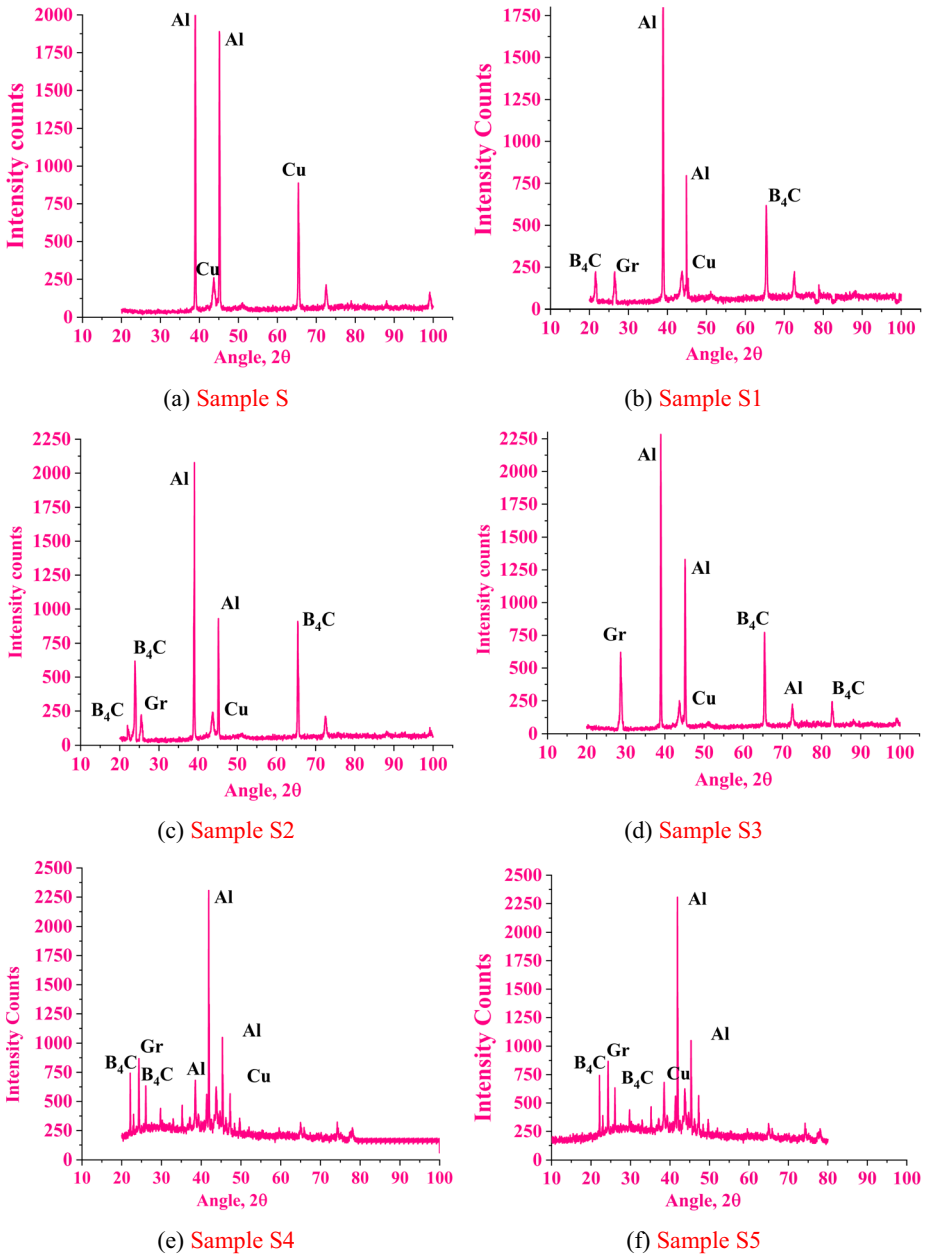

Fig. 3 XRD of sample

Sample S exhibits lower wear resistance in contrast with the hybridised sample (S1-S5). The primary reason is that the unreinforced sample S expands as the temperature rises. In addition to that, oxidation occurs at 50℃ and the wear rate of sample S has continued to grow. Oxide layer emergence decreases wear rates with greater temperature by preventing continuous metal-to-metal contact. As temperature increases, the wear resistance of the sample increases by 27%. The oxide layer on the sample surface is destroyed as a result of repeated sliding, resulting in direct metal-to-metal interaction and the exposure of new regions to the sliding disc. At lower temperature (323℃), the stability of the oxide layer is inadequate, resulting in reduced wear resistance (Fig. 6

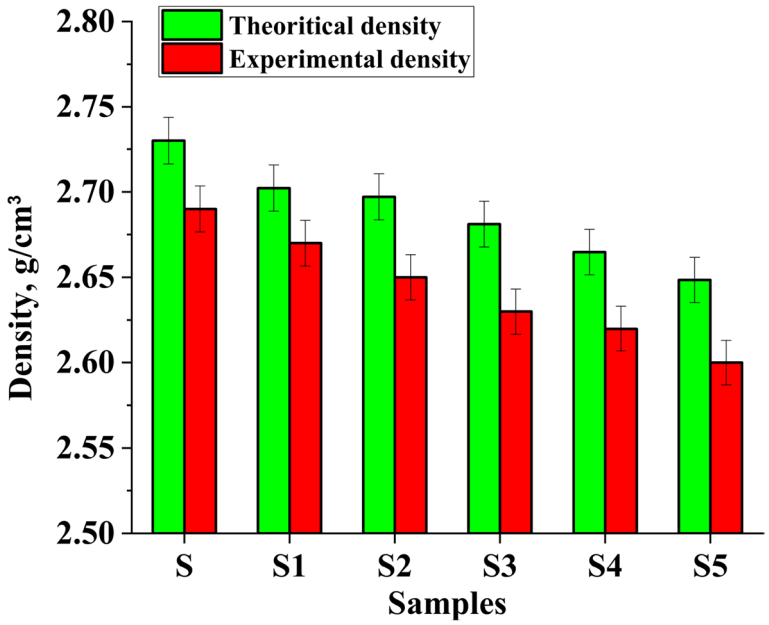

Fig. 4 Variation of density with various wt.% of B_4C and Gr

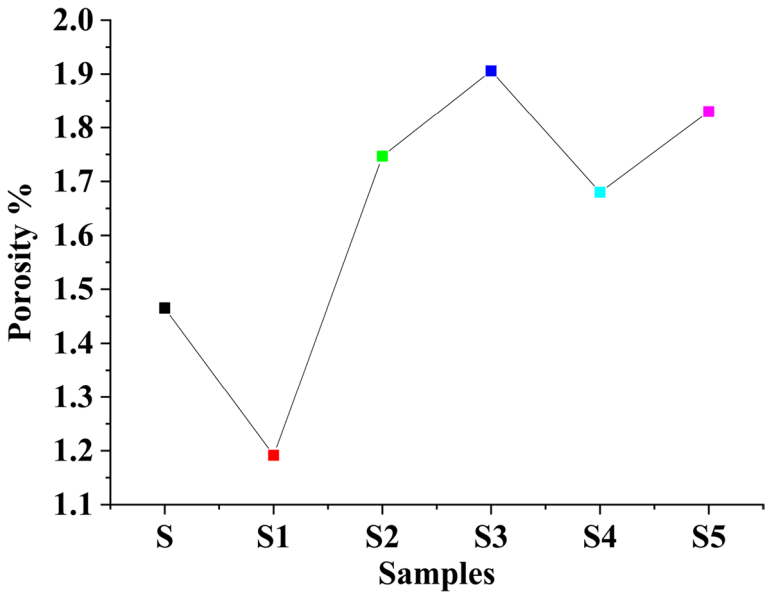

Fig. 5 Variation of porosity with various wt.% of B_4C and Gr

(a–c)). When B_4C and graphite are combined at a 3:2 ratio in Al2618, they provide excellent wear resistance (12%), in contrast with sample S. Furthermore, as the temperature rises, the wear resistance rises dramatically.

Oxide layers are ripped during sliding with steel discs due to thermal stress and compaction at higher temperatures. Fragments of the worn oxide layer were dispersed between the disc and the sample surface. Sintering of tiny wear debris happens instantly owing to the temperature and exerted pressure [27, 28].

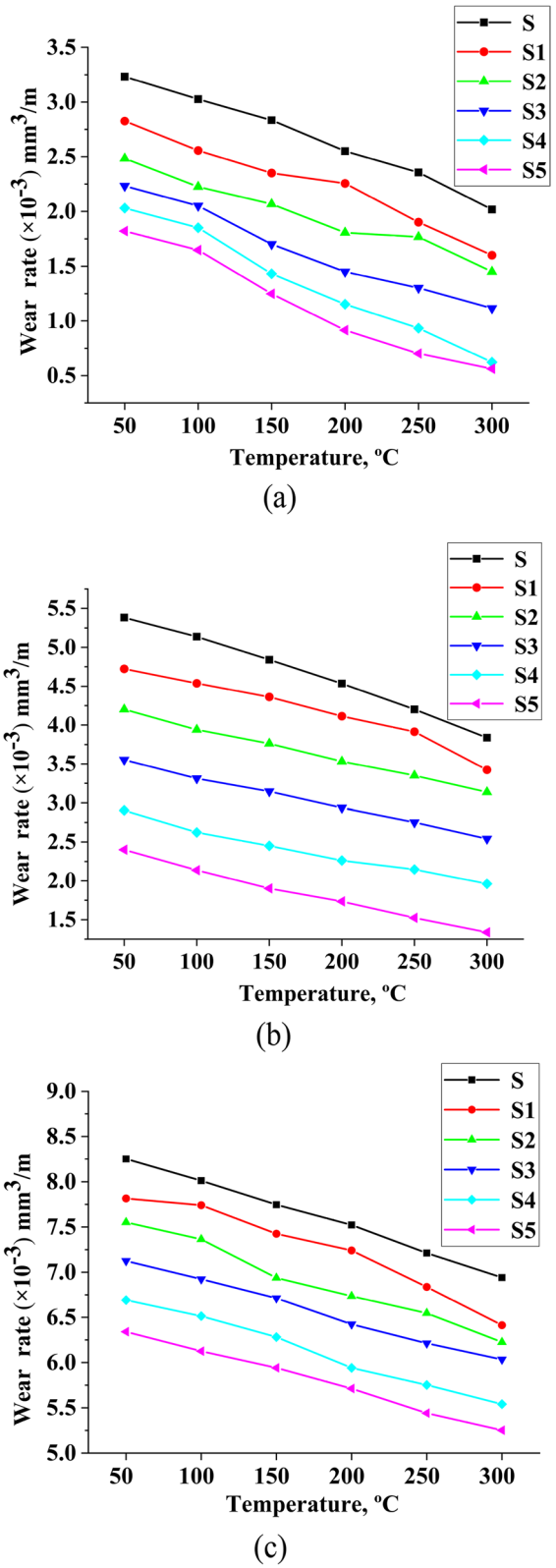

Fig. 6 Effect of temperature on the wear rate of the samples for different wt.% of reinforcement: **a** 20 N and 1.25 m/s, **b** 40 N and 2.5 m/s, and **c** 60 N and 3.75 m/s

The rate of sintering accelerates in direct proportion to the temperature at which it occurs, resulting in the formation of a solid surface known as a glaze layer. The glaze layer seeks to protect the sliding surfaces from exerted forces for a prolonged period of time and thereby reduces the wear rate. The breakdown of the glaze layer leads to the formation of an oxide layer after that the oxide layer is torn, resulting in debris. This worn debris is subjected to sintering, and the process is repeated. The wear trend shows that the glaze effect has remained unaffected at room temperature for metal and composites. Due to the presence of a thick glazed layer, S2 has considerable wear resistance (28%). Unfortunately, the formation of the glazed layer is insufficient at lower temperatures, with only 23% wear resistance observed. The durability of the glaze will be depending on the wt.% of B_4C and Gr and the thickness of the glaze layer. B_4C keeps the glazing layer stable. Dispersion strengthening and strain hardening are two factors that must be considered while describing the wear behaviour of ceramic-reinforced AMMCs. B_4C and graphite dispersion contribute to increased hybrid sample wear resistance. These particles become part of the glazed layer once they have been separated from the sample. Graphite serves as supplementary reinforcing material in HMMCs. Graphite particles create lubricity between the disc and the sample, which has the added benefit of lowering the wear rate. As demonstrated in Fig. 6**,** samples S3, S4, and S5 are of outstanding wear resistance even at higher loads [26, 29, 30].

In contrast with samples S, S4 and S5 can significantly perform at greater temperatures (300 ℃). S4 exhibits 37% wear resistance (at 50 ℃ and 20 N) and 70% (at 20 N and 300 ℃). S5 exhibits 43% wear resistance (at 50 ℃ and 20 N) and 60% (at 20 N and 300 ℃). The presence of B_4C and Gr particles can enhance the strengthening kinetics of the Al2618. The unreinforced sample S and hybridised samples (S1–S5) are sustained under similar sliding conditions up to 300 ℃; however, once the temperature rises over this point, the sample is squeezed out from the disc while the test is being conducted.

Effect of load on the wear rate of Al2618 and HMMCs

Figure 7 (a–f) depicts the impacts of applied load on the wear rate of the Al2618 and HMMCs at various conditions for all compositions ($T=50$ ℃, 100 ℃, 150 ℃, 200 ℃, 250 ℃, 300 ℃**;** $L=20$, 40, and 60 N; $S=1.25$, 2.5, 3.75 m/s; $D=800$ m). Figure 7 (a–f) concluded that the prevalence of the wear rate rises as the load increases for all samples (S-S5). The rise in wear rate is reported for all samples as the load increases from 20 to 60 N. But the wear rate was observed to fall from S to S5 while the HMMC content of refinement increased (Fig. 7 (a–f)). The growth of the wear rate complies with Archard's wear law, according to which the wear rate is linear to the applied load.

The significant rise in the wear rate was owing to the increase in the contact made between the samples and the counterface. All samples displayed essentially the same sort of wear performance at low load (20 N). Excellent interfacial bonding between the ceramic phase and the matrix and greater hardness, which leads to superior wear resistance. As the load grows, so does the varying region and degree of the worn subsurface, resulting in an increase in the quantity of the cracked brittle phase. Furthermore, a few of these broken brittle phases are released from the matrix and returned to the matrix as a consequence of the applied force, resulting in a lower contact area, which is attributable to a higher wear rate.

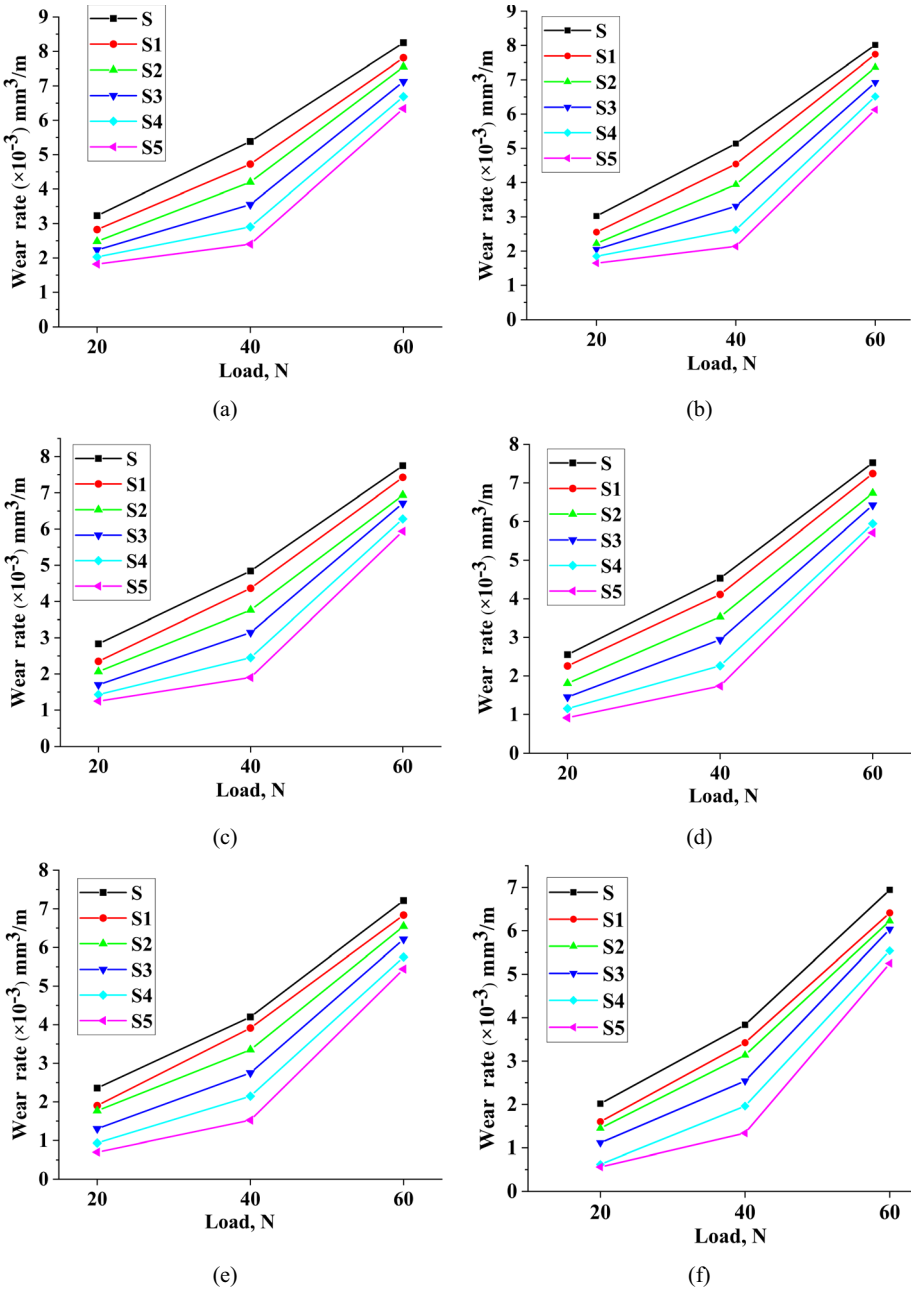

Fig. 7 Effect of load on wear rate of the samples for different wt.% of reinforcement (1.25, 2.5, and 3.75 m/s and 800 m): **a** 50 ℃, **b** 100 ℃, **c** 150 ℃, **d** 200 ℃, **e** 250 ℃, and **f** 300 ℃

Crack penetration is quicker at greater loads, and the creation of voids is hastened. The spreading cracks become progressively interconnected, producing matrix deformation and delamination. The strengthening particles serve as the primary load barrier and provide resistance to wear. From Fig. 7, it can be concluded that the wear rate for strengthened HMMCs is lowered compared to unreinforced Al2618 alloy under different load conditions. All samples (S-S5) have virtually the same sort of wear behaviour, at every load. In contrast, to sample S, the wear resistance of the hybridised sample S5 was raised

by 70% at 20 N and 300 ℃ and 19% at 60 N and 300 ℃. This is owing to the enhanced hardness (48%) of the HMMCs because of the inclusion of hard ceramic particles.

During the sliding, the sample frequently meets the steel. Upon incorporation of B_4C and Gr, particles disrupt the interference between the sample and disc. Gr works on the counter surface as a lubricant and can shape a glazed layer under temperature. B_4C and Gr are products of the glaze layer which prevent the surface contact of the sample, resulting in an increase in the HMMCs' wear resistance (S1–S5). S4 and S5 have superior wear resistance owing to the use of more Gr solid lubricants in addition to B_4C. The thickness and stability of the glaze vary according to the B_4C and Gr proportions. Thus, S4 and S5 exhibit greater wear resistance.

Effect of sliding speed on the wear rate of Al2618 and HMMCs

Figure 8 (a–f) demonstrates the impact of sliding velocities on Al2618 and HMMCs' wear rates in various conditions ($S = 1.25$ m/s, 2.5 m/s, and 3.75 m/s). All HMMCs have virtually the same sort of wear behaviour, with low speed and low temperature (1.25 m/s and 50 ℃). It has been discovered that the wear rate rises with increasing sliding speed and that this is clearly reflected in unreinforced samples. Wear resistance improves when more B_4C and Gr are added, which is notably visible in S4 and S5. As the sliding speed rises, the wear rate for sample S is raised by 86%. In the case of sample *S*, the lack of ceramic particles in the matrix led to the matrix being worn out at a quicker rate with an increased sliding speed. The increasing incorporation of B_4C and Gr boosts the wear resistance, which is particularly apparent at S4 and S5. These hard-strengthening particles were anticipated to bear a larger load between contacts even at high temperatures. It is extremely difficult to sustain larger loads for HMMCs with lower proportions of B_4C and Gr, and the load is inevitably transmitted to the Al matrix. As a result, the Al matrix is not adequately protected by these fewer reinforcing particles, which is especially noticeable in S1 and S2. In comparison to other HMMC samples, S4 and S5 demonstrate a lower wear rate, where the wear resistance increased by 49% and 37%, respectively. On the other hand, beyond a certain critical speed, the glaze layer is lost and contributes to a higher wear rate (Table 3).

Effect of temperature and load on coefficient of friction

The change of COF with temperature, with changing B_4C and Gr proportion in the Al2618 and HMMCs, is illustrated in Fig. 9a. It has been noted that COF drops for all hybridised and unhybridised samples (S-S5) with an increasing temperature. When the temperature rises from 50 to 300 ℃, the COF values drop by approximately 69%. The glaze layer on the surfaces is shown to be reliable at higher temperatures and inhibits sample wear. The glaze layer, on the other hand, degrades quickly and becomes unstable under higher loads. The shattered glaze becomes trapped between sliding surfaces, causing three-body abrasions. The cumulative effects of delamination and abrasive wear lead to extremely high wear and continue to increase the COF.

All HMMCs have virtually the same sort of COF values, with low loads (20 N). The result also suggests that the COF of the HMMCs diminishes with a rise in wt.% of B_4C and Gr particles for all loads (Fig. 9b). Additional COF-reducing factors may be

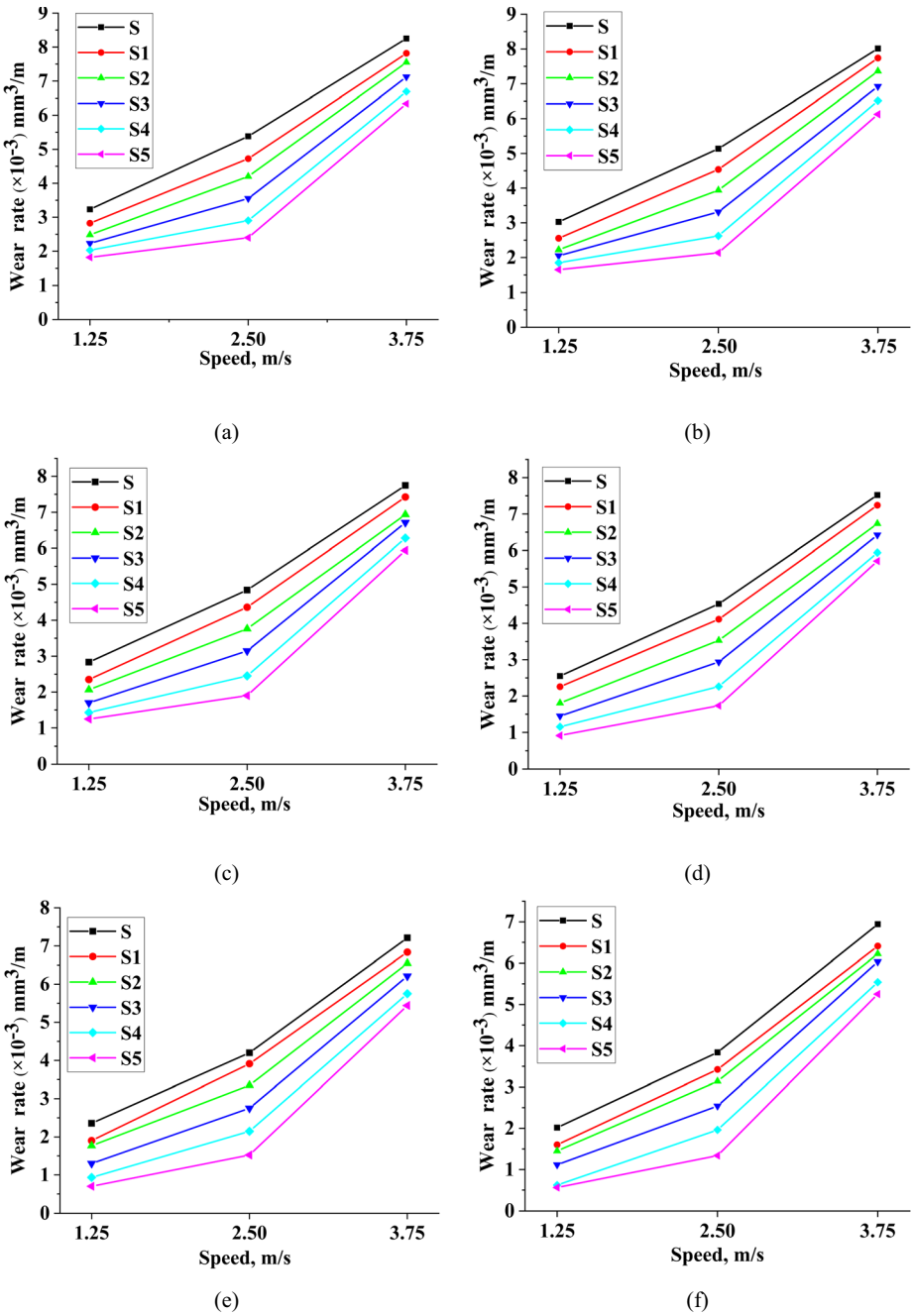

Fig. 8 Effect of speed on the wear rate of the samples for different wt% of reinforcement (20, 40, and 60 N and 800 m): **a** 50 ℃, **b** 100 ℃, **c** 150 ℃, **d** 200 ℃, **e** 250 ℃, and **f** 300 ℃

attributed to an improvement in the anti-frictional properties of strengthened particulates, with a rise in B_4C and Gr particulates in hybridised Al2618. Furthermore, the lower COF of HMMCs may be ascribed to better dispersion of ceramic particles, better bonding between Al2618 and the ceramic phase, and smaller particle sizes of B_4C and Gr [33, 34].

Table 3 Studies on wear behaviour of composites at high temperature

Author	Description	Ref.
Singh et al.	There was a higher wear rate observed, but there was an improvement in resistance at 150℃.	[7]
Straffelini et al.	Abrasion and adhesion were achieved with a load of less than 200 N. The coefficient of friction (μ) was measured to be 0.45 at a load of 200 N.	[31]
Khan et al.	The use of 20 wt.% B_4C results in a marginal increase in the transition temperature, elevating it from 262 to 274 ℃.	[10]
Zhan et al.	Characterisation of wear has been evaluated throughout a range of temperatures, specifically from 100 to 450 ℃. The utilisation of Gr particles as an effective additive for Cu-based Metal Matrix Composites (MMCs) at elevated temperatures has been seen.	[11]
Pauschitz et al.	Wear and oxidation on the process of material deterioration that occurs during sliding at elevated temperatures. The management of the glazing layer generation is contingent upon the various types of wear.	[13]
Natarajan et al.	The use of TiB2 reinforcement enhances the wear resistance of the alloy at both ambient and elevated temperatures, as compared to the alloy without any reinforcement. The prevalence of adhesive wear is most pronounced within the temperature range of 200 to 300 ℃.	[32]
Kumar et al.	Even when exposed to a temperature of 573 °K, there was no observable transition from mild to severe wear. The particle hardness of the sub-surface layer exerts a significant influence. In comparison to untreated Al6061-based AMMCs, the Al6061-T6-based AMMCs have exhibited enhanced wear resistance.	[24]

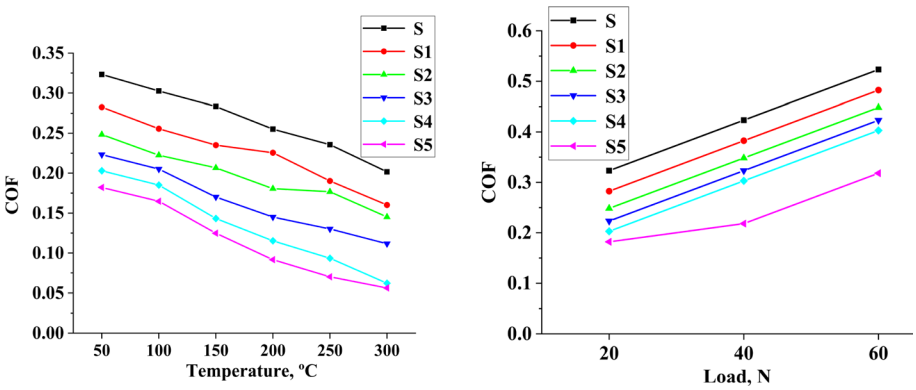

a. Effect of temperature on COF of the samples for various wt.% of reinforcement.

b. Effect of load on COF of the samples for different wt.% of reinforcement.

Fig. 9 **a** Effect of temperature on COF of the samples for various wt.% of reinforcement. **b** Effect of load on COF of the samples for different wt.% of reinforcement

Morphology of worn-out surfaces

SEM images of worn-out surfaces of unreinforced Al2618 alloy ($T = 50$ to 300 ℃, $L = 40$ N, $S = 2.5$ m/s, and $D = 800$ m) are shown in Fig. 10. In SEM pictures, it is possible to notice that adhesion is the predominant wear mechanism and that it was also found during the wear test. Figure 10 shows SEM pictures of a worn-out surface at 40 N, and the surface displays big sticky grooves. Sample S shows that at 40 N, there is micro-ploughing on the surface. At a greater load (40 N), sample S showed more surface fractures than at lower loads. This is owing to extreme plastic deformation when B_4C and Gr particles are not present. Sample S exhibits a higher wear rate at 40 N. When the load is raised from 20 to 60 N, the wear resistance decreases by 48%. The

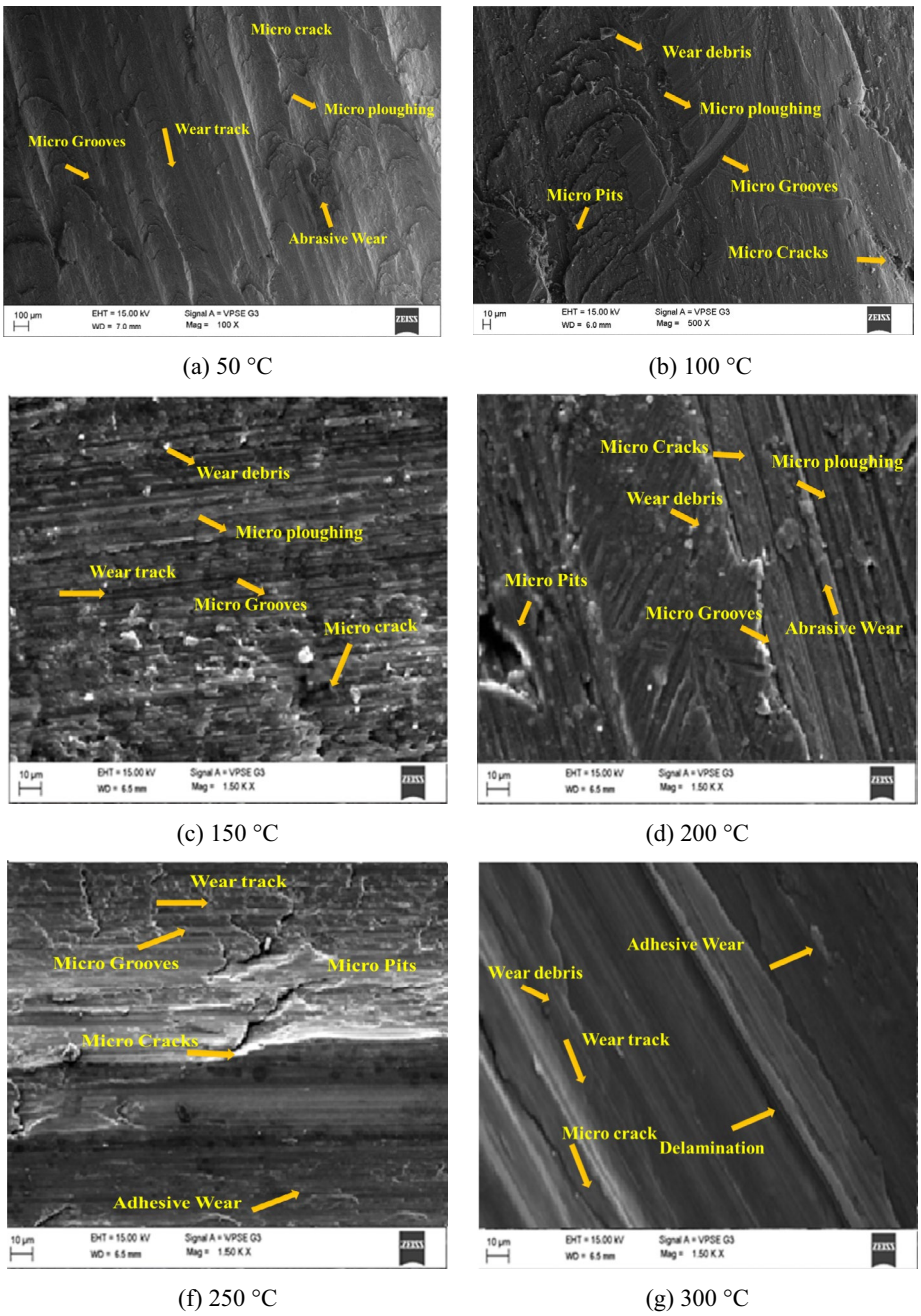

Fig. 10 Worn surface of specimen S at different temperatures

change in shape and size of the asperities under plastic deformation increases with higher depth of the ploughing marks causing more losses that have occurred on the sample surface.

The SEM micrograph of the wear track of sample S4 depicts different marks because of variation in wear. Figure 11 displays the wear track micrographs of the S4 tested at ($T=50$ to 300 ℃, $S=2.5$ m/s, $D=800$ m, and $L=40$ N). As shown in Fig. 11, the damaged asperities and some damaged area on the worn surface which is due to the

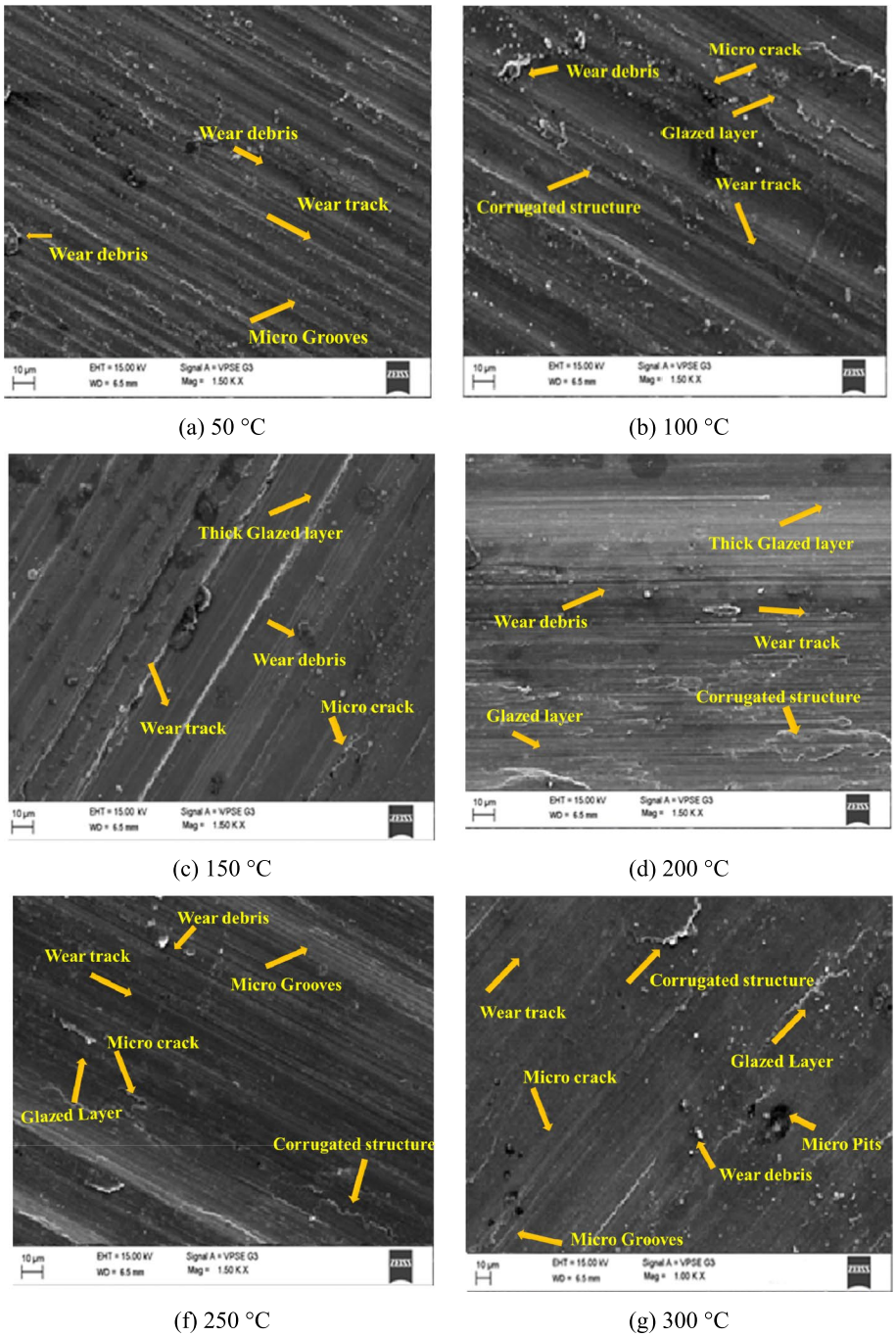

Fig. 11 Worn surface of specimen S4 at different temperatures

formation of a void around the particle are the weak spots to start the crack which ultimately led to the removal of the upper surface in terms of flake-like wear debris. This can be clearly understood because of adhesive wear. The sliding between two contact surfaces allows the asperities to penetrate the sample to form grooves. At 200 to 300 ℃, the oxidative wear is dominant which can make out from the white shiny metallic debris. The corrugated structure, as well as molten metal debris, is clearly visible. Small

plate-type debris with micro-cracks on the surface indicates the initiation of the delamination wear. In contrast, the micrograph with the wear debris at 200 to 300 ℃ shows the droplets of molten liquid of irregular shapes with rough edges. The glazed layer thickness and stability were good enough to resist wear as seen in Fig. 11. Graphite particles create lubricating films on the surface, as seen in Fig. 11 (c–f), and the arrow in Fig. 11 (d, e) illustrates that Gr flows soon on the surface. This minimises deformation in the sub-surface; therefore, no sub-surface cracks were detected on the sample surface.

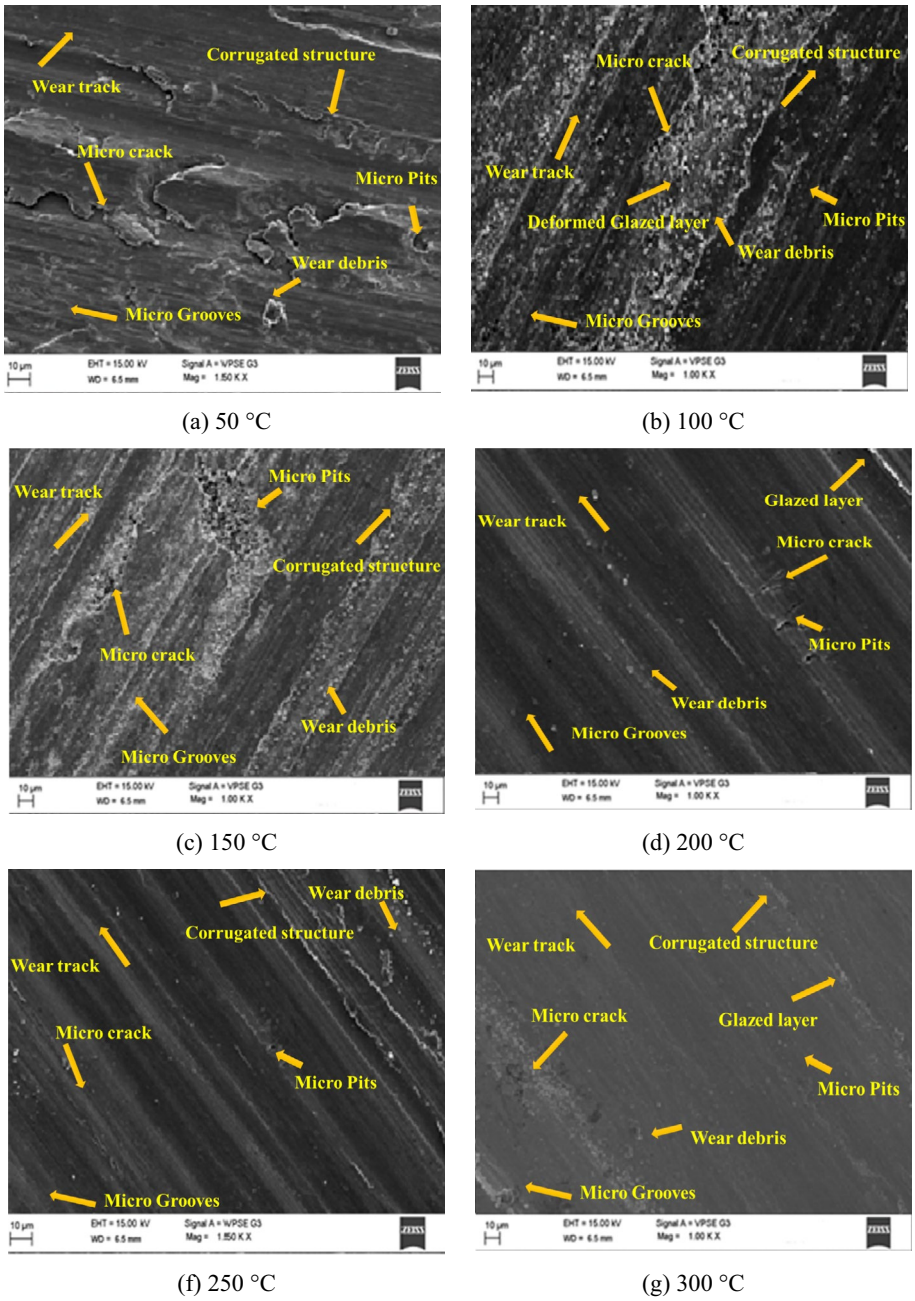

Fig. 12 Worn surface of specimen S5 at different temperatures

The SEM micrographs of the wear track of the sample S5 depict different marks because of variation in wear. Figure 12 (a–f) displays the wear track micrographs of the S5 tested at (T = 50 to 300 ℃, S = 2.5 m/s, D = 800 m, and L = 40 N). Figure 12 (b) shows that there was less damage to the area, as shown by the lack of deep grooves and the slower rate of wear. In Fig. 12 (a, b) some cracks on glazed layers of the wear tracks due to the higher applied stress on the contact surface can be seen. At higher temperatures (200 to 300 ℃), a larger delaminated area along with deeper grooves of the composite is observed as shown in Fig. 12 (d–f). Groove depth and the delaminated area also indicate the lower wear rate of the sample. The bonding between particles to the matrix is strong which is shown in the Fig. 12 (f). A larger amount of the glazed layer is formed and fills up the damaged area. The delamination area is clearly observed in the SEM micrograph.

The SEM micrograph shows that there is a lot of material flow in the direction of sliding because there is a lot of plastic deformation and fine particles are rubbing against each other. The SEM micrograph also shows some ceramic fragments that have broken off from the surface (Fig. 12 (d, e)). The increase in the size of delaminated debris that has a corrugated structure is an indication of the greater wear rate that the composites will experience under these conditions. During low-temperature wear tests showed that the material had delaminated, which was caused by the start of microcracks. This could be seen by looking at the edges of the broken pieces (50 to 150 ℃). At higher temperatures (200 to 300 ℃), wear resistance has increased as a result of the creation of a glazed layer on the worn surface of HMMC samples, as evidenced by a reduction in the delaminated area and the coverage of grooves by the glazed layer [35].

Conclusions

Based on the selection of the materials, its fabrication, and through various testing procedures, the following conclusions have been made:

- The hybrid metal matrix composites (hybrid (B_4C and Gr) Al2618 matrix composites) were successfully fabricated through the stir-casting process without agglomeration.
- The produced HMMCs have a lower density than the Al2618 alloy, which is due to the lower density of the added reinforcements.
- SEM examination of hybridised samples shows that the reinforcement particles are distributed uniformly throughout the matrix, and the XRD analysis confirms the presence of B_4C and Gr in the matrix.
- The Al2618-based HMMCs have better wear characteristics at high temperatures, making them more suitable for tribological applications at higher temperatures.

Abbreviations

Al	Aluminium
HMMCs	Hybrid metal matrix composites
MMCs	Metal matrix composites
SEM	Scanning electron microscope
XRD	X-ray diffraction
Gr	Graphite

B_4C	Boron carbide
UTS	Ultimate tensile strength
AMMCs	Aluminium metal matrix composites

Acknowledgements
Not applicable.

Authors' contributions
All authors have participated in the (a) conception and design or analysis and interpretation of the data, (b) drafting the article or revising it critically for important intellectual content, and (c) approval of the final version. All authors have read and approved the manuscript.

Funding
This research did not receive any specific grant from funding agencies in the public, commercial, and not-for-profit sectors.

Availability of data and materials
The raw/processed data required to reproduce these findings can be shared on request.

Declarations

Competing interests
The authors declare that they have no competing interests.

Received: 14 June 2023 Accepted: 28 September 2023
Published online: 11 October 2023

References

1. Sharma AK, Bhandari R, Aherwar A, Rimašauskienė R (2020) Matrix materials used in composites: a comprehensive study. Mater Today Proc 1(21):1559–1562. https://doi.org/10.1016/j.matpr.2019.11.086
2. Breval E (1995) Synthesis routes to metal matrix composites with specific properties: a review. Compos Eng 5(9):1127–1133. https://doi.org/10.1016/0961-9526(95)00048-R
3. Surappa MK (2003) Aluminium matrix composites: challenges and opportunities. Sadhana 28(1–2):319–334. https://doi.org/10.1007/BF02717141
4. Suresh S (2013) Fundamentals of metal-matrix composites. Elsevier. ISBN: 9780080523712.
5. Ahmed A, Wahab MS, Raus AA, Kamarudin K, Bakhsh Q, Ali D (2016) Mechanical properties, material and design of the automobile piston: an ample review. Indian J Sci Technol 9(36):1–7. https://doi.org/10.17485/ijst/2016/v9i36/102155
6. Macke A, Schultz BF, Rohatgi P (2012) Metal matrix composites. Adv Mater Processes 170(3):19–23. https://doi.org/10.29252/jcc.2.2.3
7. Singh J, Alpas AT (1996) High-temperature wear and deformation processes in metal matrix composites. Metall Mater Trans A 27(10):3135–3148. https://doi.org/10.1007/BF02663864
8. Bonollo F, Ceschini L, Garagnani GL (1997) Mechanical and impact behaviour of (Al 2 O 3) p/2014 and (Al 2 O 3) p/6061 Al metal matrix composites in the 25–200° C range. Appl Compos Mater 4(3):173–185. https://doi.org/10.1007/BF02481779
9. Xia X, McQueen HJ (1997) Deformation behaviour and microstructure of a 20% Al_2O_3 reinforced 6061 Al composite. Appl Compos Mater 4(6):333–347. https://doi.org/10.1007/BF02481398
10. Khan KB, Kutty TR, Surappa MK (2006) Hot hardness and indentation creep study on Al–5% Mg alloy matrix–B_4C particle reinforced composites. Mater Sci Eng, A 427(1–2):76–82. https://doi.org/10.1016/j.msea.2006.04.015
11. Zhan Y, Zhang G (2006) The role of graphite particles in the high-temperature wear of copper hybrid composites against steel. Mater Des 27(1):79–84. https://doi.org/10.1016/j.matdes.2004.08.019
12. Zhang Hui, He Yusong, Li Luoxing (2008) Tensile deformation and fracture behavior of spray-deposition 7075/15SiCp aluminum matrix composite sheet at elevated temperatures. Mater Charac 59(8):1078–1082. https://doi.org/10.1016/j.matchar.2007.08.027
13. Pauschitz A, Roy M, Franek F (2008) Mechanisms of sliding wear of metals and alloys at elevated temperatures. Tribol Int 41(7):584–602. https://doi.org/10.1016/j.triboint.2007.10.003
14. Kumar PRS, Kumaran S, Srinivasa Rao T, Natarajan S (2010) High temperature sliding wear behavior of press-extruded AA6061/fly ash composite. Elsevier Mater Sci Eng A 527(6):1501–1509. https://doi.org/10.1016/j.msea.2009.10.016
15. Kumar S, SubramanyaSarma V, Murty BS (2010) High temperature wear behavior of Al–4Cu–TiB2 in situ composites. Wear 268(11–12):1266–1274. https://doi.org/10.1016/j.wear.2010.01.022
16. Ballupete Nagaraju S, Kodigarahalli Somashekara M, Puttegowda M, Manjulaiah H, Kini CR, Channarayapattana VV (2022) Effect of B4C/Gr on hardness and wear behavior of Al2618 based hybrid composites through taguchi and artificial neural network analysis. Catalysts 12(12):1654. https://doi.org/10.3390/catal12121654
17. Chikkegouda SP, Gurudath B, Sharath BN, Karthik S, Mahale RS (2022) Mechanical and tribological characteristics of aluminium 2618 matrix composite reinforced with boron carbide. Biointerface Res Appl Chem 12:4. https://doi.org/10.33263/BRIAC124.45444556

18. Sharath BN, Venkatesh CV, Afzal A, Aslfattahi N, Aabid A, Baig M, Saleh B (2021) Multi ceramic particles inclusion in the aluminium matrix and wear characterization through experimental and response surface-artificial neural networks. Materials 14(11):2895. https://doi.org/10.3390/ma14112895
19. Madhu KS, Sharath BN, Venkatesh CV, Pradeep DG (2021) Evaluation of mechanical properties of ceramic reinforced aluminium-7029 hybrid composite. In IOP Conference Series: Materials Science and Engineering (Vol. 1189, No. 1, p. 012019). IOP Publishing. https://doi.org/10.1088/1757-899X/1189/1/012019
20. Sharath BN, Jeevan TP, Baig MA, Ashrith HS, Afzal A, Reddy AR (2021) Machinability studies on boron carbide and graphite reinforced aluminium hybrid composites. Mater Today Proc 1(46):8734–8741. https://doi.org/10.1016/j.matpr.2021.04.036
21. Madhu KS, Venkatesh CV, Sharath BN, Karthik S (2021) Effect of boron carbide on wear resistance of graphite containing Al7029 based hybrid composites and its dry sliding wear characterization through experimental, response surface method and ANOVA. Tribol Finn J Tribol 38(3–4):48–60. https://doi.org/10.30678/fjt.111905
22. Sharath BN, Karthik S, Pradeep DG, Madhu KS, Venkatesh CV (2022) Machinability studies on boron carbide and graphite reinforced Al7029-based hybrid composites. In Materials, Design and Manufacturing for Sustainable Environment: Select Proceedings of ICMDMSE 2022. Springer Nature Singapore, Singapore, pp 511–522. https://doi.org/10.1007/978-981-19-3053-9_38
23. Madhu KS, Venkatesh CV, Sharath BN, Karthik S (2022) Characterization and evaluation of mechanical properties of Al-Zn based hybrid metal matrix composites. Appl Sci Eng Prog 16(1):58041. https://doi.org/10.14416/j.asep.2022.03.008
24. Sharath BN, Madhu KS, Venkatesh CV (2019) Experimental study on dry sliding wear behaviour of Al-B4C-Gr metal matrix composite at different temperatures. Appl Mech Mater 895:96–101. https://doi.org/10.4028/www.scientific.net/AMM.895.96. Trans Tech Publications Ltd
25. Shekar AC, Pathinettampadian G, Suthan R, De Poures MV, Althahban S, Mousa S, Qahtani F, Jazaa Y, Girma B (2022) Optimization on wear rate of AA2219/nanographite/TiB2/Si3N4 hybrid composites using Taguchi process. J Nanomater 9:2022. https://doi.org/10.1155/2022/1814623
26. Sharma S, Gupta R, Nanda T, Pandey OP (2021) Influence of two different range of sillimanite particle reinforcement on tribological characteristics of LM30 based composites under elevated temperature conditions. Mater Chem Phys 15(258):123988. https://doi.org/10.1016/j.matchemphys.2020.123988
27. Sharath BN, Venkatesh CV (2021) Study on Effect of boron carbide, aluminium oxide and graphite on dry sliding wear behaviour of aluminium based metal matrix composite at different temperature. Tribol Finn J Tribol 38(1–2):35–46. https://doi.org/10.30678/fjt.99931
28. Sharath BN, Madhu KS, Pradeep DG, Venkatesh CV (2021) Tribological Suitability of aluminium hybrid composite above atmospheric temperature. In IOP Conference Series: Materials Science and Engineering (Vol. 1189, No. 1, p. 012018). IOP Publishing. https://doi.org/10.1088/1757-899X/1189/1/012018
29. Gupta R, Nanda T, Pandey OP (2022) Tribological properties of hybrid aluminium matrix composites reinforced with boron carbide and ilmenite particles for brake rotor applications. Arch Civ Mech Eng 23(1):47. https://doi.org/10.1007/s43452-022-00569-
30. Gupta R, Nanda T, Pandey OP (2022) Effect of high operating temperatures on the wear characteristics of boron carbide and ilmenite reinforced LM13 alloy-based composites. J Tribol 144(10):101703. https://doi.org/10.1115/1.4054318
31. Straffelini G, Pellizzari M, Molinari A (2004) Influence of load and temperature on the dry sliding behaviour of Al-based metal-matrix-composites against friction material. Elsevier-Wear 256(7–8):754–763. https://doi.org/10.1016/S0043-1648(03)00529-5
32. Natarajan S, Narayanasamy R, Babu SPK, Dinesh G, Anil Kumar B, Sivaprasad K (2009) Sliding wear behavior of Al 6063/TiB2 in situ composites at elevated temperatures. Mater Des 30(7):2521–2531. https://doi.org/10.1016/j.matdes.2008.09.037. Elsevier
33. Kaibyshev R, Sitdikov O, Mazurina I, Lesuer DR (2002) Deformation behavior of a 2219 Al alloy. Mater Sci Eng A 334(1–2):104–113. https://doi.org/10.1016/S0921-5093(01)01777-4
34. Onoro J, Salvador MD, Cambronero LE (2009) High-temperature mechanical properties of aluminium alloys reinforced with boron carbide particles. Mater Sci Eng A 499(1–2):421–426. https://doi.org/10.1016/j.msea.2008.09.013
35. Mousavi Abarghouie SMR, Seyed Reihani SM (2010) Investigation of friction and wear behaviors of 2024 Al and 2024 Al/SiCp composite at elevated temperatures. J Alloys Compd 501(2):326–332. https://doi.org/10.1016/j.jallcom.2010.04.097. Elsevier

Publisher's Note